# Laboratory Simulation of the Atmospheric Boundary Layer

J. E. CERMAK*
*Colorado State University, Fort Collins, Colo.*

**Similarity criteria are given for micro-, small-, and meso-scale motion of the atmospheric boundary layer. Requirements for simulation of dispersion of passive contaminants in the atmosphere are discussed. The characteristic features of a unique meteorological wind tunnel with a capability for simulating thermally stratified boundary layers are described. Mean wind speed, mean temperature and turbulence statistics measured in this laboratory facility are found to be similar to corresponding data obtained from measurements in the atmosphere. Examples of simulated dispersion over a variety of surface features including urban areas and complex topography are described.**

## Nomenclature

$b$ = Batchelor constant (approx. 0.4)
$C_p$ = specific heat at constant pressure
$f(K)$ = energy spectrum of longitudinal turbulence component
$g$ = gravitational acceleration
$h$ = source height
$H$ = dimensionless source height ($h/z_o$)
$k$ = thermal conductivity of fluid
$k_c$ = diffusivity of contaminant in air
$K$ = wave number
$K_c$ = eddy diffusivity for contaminant
$K_M$ = eddy diffusivity for momentum
$L$ = reference length
$P$ = deviation of mean pressure from static reference
$t$ = time
$T$ = instantaneous temperature
$\bar{T}_w$ = mean temperature at $z = 0$
$\Delta\bar{T}$ = $\bar{T} - \bar{T}_w$
$(\Delta\bar{T})_o$ = $\bar{T}_o - \bar{T}_w$
$u_i$ = $i$th component of instantaneous velocity
$\bar{U}_i$ = $i$th component of mean velocity
$w'$ = vertical velocity fluctuation
$x_i$ = $i$th space coordinate
$z$ = vertical coordinate
$z_o$ = roughness length
$\delta$ = boundary-layer thickness
$\delta_T$ = thermal boundary-layer thickness
$\delta_{ij}$ = Kronecker delta
$\epsilon$ = energy dissipation rate per unit of mass
$\epsilon_{ijk}$ = permutation tensor
$\zeta$ = dimensionless height ($z/z_o$)
$\rho$ = mass density
$\theta'$ = fluctuation of temperature from mean
$\kappa$ = von Kármán constant
$\nu$ = kinematic viscosity
$\xi$ = dimensionless distance downwind ($x/z_o$)
$\phi$ = dissipation function
$\chi$ = concentration of contaminant
$\Omega$ = angular velocity

*Subscripts*

$(\ )_g$ = quantity at geostrophic level
$(\ )_o$ = reference quantity

*Superscripts*

$(\ )^*$ = nondimensional quantity
$\overline{(\ )}, \langle\ \rangle$ = time average
$(\ )'$ = instantaneous fluctuation from time average

Presented as Paper 70-751 at the AIAA 3rd Fluid and Plasma Dynamics Conference, Los Angeles, Calif., June 29–July 1, 1970; submitted August 10, 1970; revision received April 29, 1971. The research results and facilities of the Fluid Dynamics and Diffusion Laboratory referred to were derived primarily through support provided by the following contracts and grants: AF-19(604)-1706, DA-36-039-SC-80371, PHS AP 0091-01-06, NSF G-4799, DA-AMC-28-043-64-G-9, DA-AMC-28-043-65-G20, and N123 (61756)34361ABMR. Project THEMIS, Contract N00014-68-A-0493-0001, provided support for preparation of this paper.

* Professor-in-Charge, Fluid Mechanics Program. Associate Fellow AIAA.

Subject Index Topics: Atmospheric, Space, and Oceanographic Sciences, Boundary Layers and Convective Heat Transfer-Turbulent; Research Facilities and Instrumentation.

## I. Introduction

ESSENTIALLY all the activities of man are influenced by atmospheric motions from ground level up to a few thousand feet in altitude. This layer, the atmospheric boundary layer, is the region in which major exchanges of heat, mass and momentum between the Earth's surface and atmosphere occur. Consequently, a good knowledge of how mean winds and turbulence characteristics are distributed vertically and horizontally is necessary if air-pollution concentrations and wind forces on structures—two particularly important environmental problems—are to be predicted with reasonable certainty.

Atmospheric boundary layers are complicated by the combined influences of the Earth's rotation, buoyancy forces, surface drag forces, and the geometry of topographic features. The Coriolis acceleration results in the mean wind direction turning to the right with increasing height (northern hemisphere) at a turning rate which depends upon the vertical distribution of eddy viscosity and density. Lettau and Dabberdt[1] by allowing the mean wind direction to be different than the direction of mean shear at a point have related turning rates to realistic eddy-viscosity distributions.

During the last two decades intensive studies of the atmospheric surface layer, the lower 100–200 ft of the atmosphere where vertical fluxes of momentum and heat are nearly constant, have been made to determine the effects of temperature stratification and surface roughness on flow characteristics. Good reviews of these efforts have been presented by Lumley and Panofsky[2] and Monin and Yaglom.[3] Most of these studies have been confined to uniform boundary temperature and roughness of heights small compared to the surface layer depth on plane surfaces. However, Cermak and Arya[4] have emphasized the need to consider the effects of nonuniform boundary temperature and roughness, roughness heights equal to and exceeding the surface layer depth, and boundary surfaces made nonplanar by topographic features. This need is particularly apparent when flows over urban areas,[5] forested areas[6] and mountainous or hilly terrain[7] must be considered.

Analysis to the extent of similarity reasoning by Monin and Obukhov[8] has been fruitful only in the particularly simple case of surface layers with planar homogeneity of the

flow statistics. As a result, field and laboratory studies have become the primary source of our knowledge on atmospheric boundary layers. The increasing need to study environmental problems in areas of complex boundary conditions has motivated serious efforts to simulate atmospheric boundary layers in the laboratory.[4,9–13]

Simulation of the atmospheric boundary layer in an exact sense does not appear to be possible. However, comparisons of data obtained in appropriate wind tunnels with corresponding atmospheric data have shown good similarity despite relaxation of requirements for exact simulation. The purpose of this paper is to review requirements for atmospheric boundary-layer simulation, describe facilities which have been designed for this purpose and to present comparisons of different types of flow and diffusion data taken from the laboratory and the field. Permissible relaxation of similarity requirements for both flow characteristics and diffusion are examined for micro-, small-, and meso-scale phenomena; i.e., approximately $10^{-3}$–$10^{1}$, $10^{1}$–$10^{4}$, and $10^{4}$–$10^{5}$ m, respectively.

## II. Similarity Criteria

The general requirements for similarity of atmospheric boundary layers may be obtained by inspection of the governing equations—statements of conservation of mass, momentum and energy. This will be accomplished by scaling the pertinent dependent and independent variables to form a dimensionless system of equations. Similarity criteria for flow characteristics and diffusion are then presented for micro-, small-, and meso-scale flows subject to specified restrictions.

### General Similarity Requirements

General similarity of two flow systems requires geometric similarity, kinematic similarity, dynamic similarity, thermal similarity, and similarity of boundary conditions. If geometric similarity is preserved through use of a common length scale for vertical and horizontal dimensions, the conservation of mass equation

$$\partial\rho/\partial t + \partial(\rho u_i)/\partial x_i = 0 \tag{1}$$

remains invariant when transformed to dimensionless form. Geometric similarity will be considered to exist for all cases discussed in this paper in which urban or topographic boundary features exist. Therefore, the physical requirement of mass conservation is satisfied as will be the requirement for kinematic similarity if the other similarity requirements are met.

Criteria for dynamic similarity are given by the momentum conservation equations (equations of motion)

$$\frac{\partial\bar{U}_i}{\partial t} + \bar{U}_j\frac{\partial\bar{U}_i}{\partial x_j} + 2\epsilon_{ijk}\Omega_j\bar{U}_k = -\frac{1}{\rho_o}\frac{\partial\bar{P}}{\partial x_i} - \frac{\Delta\bar{T}}{\bar{T}_o}g\delta_{i3} + \nu_o\frac{\partial^2\bar{U}_i}{\partial x_k\partial x_k} + \frac{\partial\langle -u_j'u_i'\rangle}{\partial x_j} \tag{2}$$

Equation 2 is the time averaged equation of motion in which instantaneous dependent variables are represented as a mean value plus a fluctuation from the mean and the Boussinesq approximation has been made to express the effect of temperature stratification upon the body force. The Boussinesq approximation limits Eq. 2 to flows in which $\Delta\bar{T} \ll \bar{T}_o$ and results in $\bar{P}$ being the departure of the mean pressure from the hydrostatic pressure for an atmosphere of density $\rho_o$.

A nondimensional form of Eq. 2 is obtained by scaling all variables as follows:

$$\bar{U}_i^* = \bar{U}_i/U_o; \quad (u_i')^* = u_i'/U_o; \quad x_i^* = x_i/L_o$$

$$t^* = tU_o/L_o; \quad \Omega_j^* = \Omega_j/\Omega_o; \quad \bar{P}^* = \bar{P}/\rho_o U_o^2$$

$$\Delta\bar{T}^* = \Delta\bar{T}/(\Delta\bar{T})_o; \quad g^* = g/g_o$$

The dimensionless expression becomes upon dividing by $U_o^2/L_o$

$$\frac{\partial\bar{U}_i^*}{\partial t^*} + \bar{U}_j^*\frac{\partial\bar{U}_i^*}{\partial x_j^*} + \left[\frac{L_o\Omega_o}{U_o}\right]2\epsilon_{ijk}\Omega_j^*\bar{U}_k^* = -\frac{\partial\bar{P}^*}{\partial x_i^*} - \left[\frac{\Delta\bar{T}_o}{\bar{T}_o}\frac{L_o g_o}{U_o^2}\right]\Delta\bar{T}^* g^*\delta_{i3} + \left[\frac{\nu_o}{U_o L_o}\right]\frac{\partial^2\bar{U}_i^*}{\partial x_k^*\partial x_k^*} + \frac{\partial\langle -u_i'u_j'\rangle^*}{\partial x_j^*} \tag{3}$$

Consequently, exact dynamic similitude requires that three dimensionless parameters formed from the scaling factors be equal for the two flow systems. These dimensionless parameters are commonly known by the following names:

| | |
|---|---|
| Reynolds number | $Re = U_o L_o/\nu_o$ |
| bulk Richardson number | $Ri = [(\Delta\bar{T})_o/T_o](L_o/U_o^2)g_o$ |
| Rossby number | $Ro = U_o/L_o\Omega_o$ |

Requirements for thermal similarity may be obtained by inspection of the statement for conservation of energy

$$\frac{\partial\bar{T}}{\partial t} + \bar{U}_i\frac{\partial\bar{T}}{\partial x_i} = \left[\frac{k_o}{\rho_o C_{p_o}}\right]\frac{\partial^2\bar{T}}{\partial x_k\partial x_k} + \frac{\partial\langle -\theta' u_i'\rangle}{\partial x_i} + \frac{\phi}{\rho_o C_{p_o}} \tag{4}$$

where $\phi$ is the dissipation function. Using a temperature scale of $(\Delta\bar{T})_o$, a nondimensional form of Eq. 4 may be expressed as follows:

$$\frac{\partial\bar{T}^*}{\partial t^*} + \bar{U}_i^*\frac{\partial\bar{T}^*}{\partial x_i} = \left[\frac{k_o}{\rho_o C_{p_o}\nu_o}\right]\left[\frac{\nu_o}{L_o U_o}\right]\frac{\partial^2\bar{T}^*}{\partial x_k^*\partial x_k^*} + \frac{\partial\langle -\theta' u_i'\rangle^*}{\partial x_i^*} + \left[\frac{\nu_o}{U_o L_o}\right]\left[\frac{U_o^2}{C_{p_o}(\Delta\bar{T})_o}\right]\phi^* \tag{5}$$

Thus, the following additional similarity parameters are introduced:

$$\text{Prandtl number} \qquad Pr = \nu_o/(k_o/\rho_o C_{p_o})$$

and

$$\text{Eckert number} \qquad Ec = U_o^2/C_{p_o}(\Delta\bar{T})_o$$

When air is used in the model for simulating the atmospheric boundary layer the Prandtl numbers are automatically equal. The similarity does not depend strongly upon the Eckert number until the flow speeds approach the speed of sound; therefore, this requirement is relaxed.

In addition to making the foregoing equations similar by requiring equality of corresponding similarity parameters for two flow systems, the boundary conditions must be similar if the two systems are to behave in a similar manner. These boundary conditions include distributions of temperature and roughness over the area of interest, the longitudinal pressure variation $\partial\bar{P}/\partial x$, and the vertical temperature and velocity distribution of the approaching flow. The last requirement places special demands upon laboratory facilities to be used for simulation of the atmospheric boundary layer.

In summary, the general criteria for similarity of atmospheric boundary layers are the following: 1) undistorted scaling of boundary geometry (geometric similarity); 2) Reynolds number equality; 3) bulk Richardson number equality; 4) Rossby number equality; 5) Prandtl number equality; and 6) boundary-condition similarity (including approach flow, surface temperature, surface roughness and $\partial\bar{P}/\partial x$). These requirements do not include similarity for radiative transfer of energy to and from the air-contaminant mixture or energy exchange produced by phase changes of

air-borne water. Therefore, the effects of these phenomena are excluded from further consideration in this discussion.

Unfortunately, laboratory facilities currently in use for simulating atmospheric boundary layers cannot obtain Rossby number equality. Therefore, the following development will be strictly applicable only to flow conditions for which effects of the Earth's rotation are negligible.

### Micro-Scale Similarity

When the surface is essentially plane, surface roughness and temperature are uniform and roughness elements are small compared to the surface-layer thickness, the surface-layer flow statistics exhibit planar-homogeneity and the vertical fluxes of momentum and heat are sensibly constant. In this case, Monin and Obukhov[8] assume that variables affecting the flow structure are height above the boundary $z$, fluid density $\rho$, surface shear stress $\tau_o$, surface heat flux $H_o$, and a stability parameter $g/\bar{T}_o$. These variables may be grouped to give the following scales for velocity, temperature and length in the atmospheric surface layer:

$$\text{shear velocity} \quad u_* = (\tau_o/\rho)^{1/2} \tag{6}$$

$$\text{friction temperature} \quad T_* = -H_o/(\rho C_p \kappa u^*) \tag{7}$$

$$\text{Monin-Obukhov length} \quad L = -u_*{}^3/[(\kappa g/\bar{T}_o)H_o/\rho C_p] \tag{8}$$

The arguments leading to these scaling factors tacitly assume that the flow is fully turbulent and that transport by molecular motions is negligible. Similarity based on these scaling factors is found to exist for flow quantities which are not affected substantially by meso-scale disturbances passing through the flow.

When the thermal stability does not depart strongly from neutral stability, the dimensionless wind shear $(\kappa z/u_*)(\partial\bar{U}/\partial z)$ and temperature gradient $(z/T_*)(\partial\bar{T}/\partial z)$ may be approximated by a linear function of $z/L$.[3,14] This formulation leads to the following log-linear distribution forms which will be used to compare laboratory and field data:

$$\bar{U}(z) - \bar{U}(z_{ref}) = u_*/\kappa[\ln(z/z_{ref}) + B_U(z - z_{ref})/L] \tag{9}$$

$$\bar{T}(z) - \bar{T}(z_{ref}) = T_*[\ln(z/z_{ref}) + B_T(z - z_{ref})/L] \tag{10}$$

These distributions reduce to well known logarithmic profiles for neutral stability ($L \to \infty$).

On the basis of Monin-Obukhov similarity, turbulence statistics in the surface layer can be scaled by the scaling factors expressed by Eqs. (6–8). In particular, the standard deviation of vertical velocity fluctuations may be expressed in the form

$$\langle w'^2\rangle^{1/2}/u_* = \phi_1[z/L] \tag{11}$$

This formulation will be used to compare measurements made in the laboratory and in the atmosphere.

At high Reynolds numbers Kolmogorov[15] makes the hypothesis that a high wave number range exists in the turbulence spectrum which is governed by the kinematic viscosity $\nu$ and the energy dissipation $\epsilon$. The corresponding length and velocity scales are $(\nu^3/\epsilon)^{1/4}$ and $(\nu\epsilon)^{1/4}$, respectively. These scaling factors provide a basis for comparing turbulence spectra for similarity. For example, one-dimensional longitudinal turbulence spectra can be related as follows:

$$[\langle u'^2\rangle f(K)]/(\epsilon\nu^5)^{1/4} = \phi_2[K(\nu^3/\epsilon)^{1/4}] \tag{12}$$

where $K$ is the wave number.

### Small-Scale Similarity

The similarities outlined in the preceding section were essentially local in nature and refer to the micro-structure. This perspective must be expanded in scale, say up to a few miles, if flow and diffusion over urban areas are to be considered. The general similarity criteria previously stated are applicable; however, more precise similarity statements are not available excepting for diffusion within a surface layer when planar homogeneity exists. In this special case, the hypothesis of Lagrangian similarity[16] is useful.

The small-scale category of flows include flow over cities where the surface roughness is extensive in height and non-uniform in distribution. Here, the atmospheric surface layer concept no longer exists in the Monin-Obukhov sense but is replaced by a flow structure which is almost entirely determined by the geometry of a particular city. When the structures, as in the usual case, are of a block form with sharp edges, a relaxation of the Reynolds number requirement for similarity is possible. The equality of Reynolds numbers is replaced by a minimum Reynolds number for the scaled down model which insures invariance of the flow pattern or the drag coefficient for a representative structure. This requirement, equality of a Richardson number and the existence of a boundary-layer thickness for the approaching flow equal to a scaled-up height of approximately 1500 ft gives a practical set of rules for satisfactory simulation of flow and dispersion within a city complex. The studies of Jensen[17] tend to substantiate this statement.

Vertical distributions of mean wind speed over cities in strong winds are found to be rather well described by some power of the height.[18] A common form, made dimensionless by scaling with the gradient wind speed for $U_g$ and the gradient wind elevation $z_g$, is as follows:

$$\bar{U}/U_g = (z/z_g)^p \tag{13}$$

For extremely rough cities $p$ approaches 0.5. This result can be interpreted to mean that the intense mixing produces an almost constant eddy viscosity in the boundary layer to give a profile similar to fully developed laminar flow (constant molecular viscosity) in plane Poiseuille flow.

In the event boundary conditions are uniform over a plane surface and the flow has planar homogeneity, the decay of maximum ground-level concentration with distance downwind from a source may be predicted. This becomes possible through use of the Lagrangian similarity hypothesis which states that for a marked particle which is at $z = h$ when $t = 0$, the statistical properties of particle motion at time $t$ depend only upon $u_*$ and $t - t_v$ when $t$ is of order $h/u_*$ or larger, where $t_v$ is a virtual time origin of magnitude of order $h/u_*$. Setting $\chi \propto \chi^m$, Cermak[16] showed that for a continuous point source the exponent $m_{cp}$ varies as follows:

$$m_{cp} = -(\kappa b\xi)[(1 + 2\log\zeta)/\zeta\log\zeta] \tag{14}$$

with

$$\kappa b\xi = \zeta\log\zeta - (\zeta - H) + (b - 1)H\log H$$

Equation 14 applies only if the mean velocity profile is logarithmic in form and the stability is neutral.

### Meso-Scale Similarity

For meso-scales from about 5–50 miles in extent, simulation of mean flow and advective dispersion is best achieved when the flow is stably stratified and the surface is highly irregular because of complex terrain. Only this case will be considered here.

With existing wind tunnels, regions of meso-scale extent must be reduced in scale by a factor of approximately $10^4$. At this scale reduction, Richardson number equality can be maintained; however, for stably stratified flow the low wind speeds and large temperature differences result in laminar flow over the model.[19] The following development gives a basis for similarity of laminar mean flow over a small scale model and turbulent mean flow over the prototype.

Suppose that geometric similarity, Richardson number similarity and boundary condition similarity exist. Reynolds

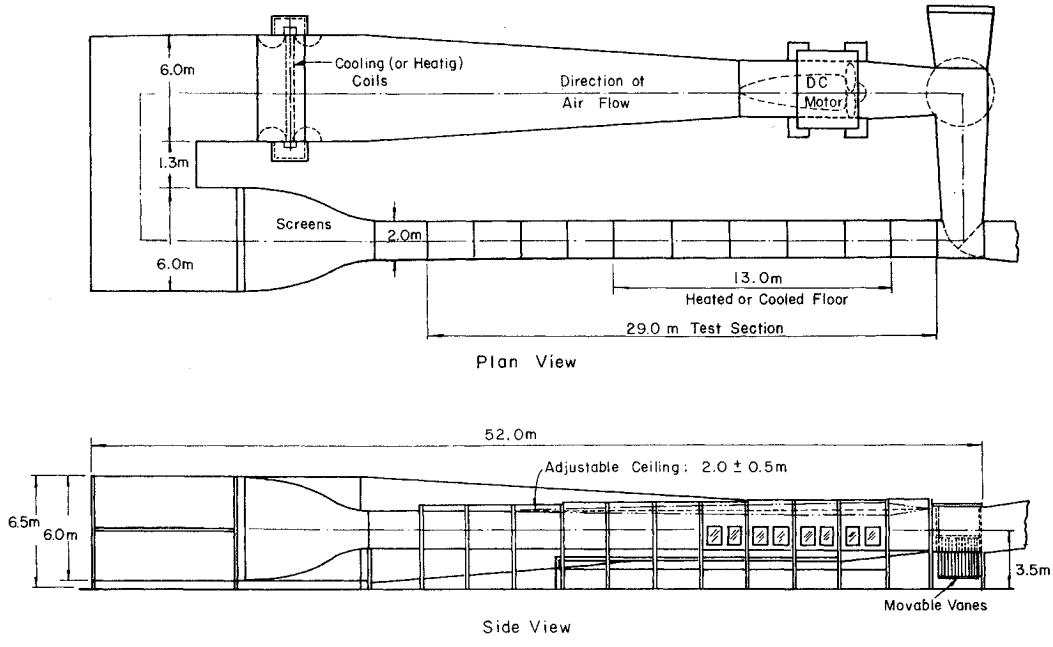


**Fig. 1 Meteorological wind tunnel.**

number equality may be examined by a study of the last two terms in Eq. 3. For this purpose, the Reynolds stresses $-\rho\langle u_i'u_j'\rangle$ are approximated by $K_M\partial\bar{U}_i/\partial x_j$; therefore, the last two terms of Eq. 3 become

$$[(\nu_o/U_oL_o) + (K_M/U_oL_o)]\partial^2\bar{U}_i^*/\partial x_k^*\partial x_k^*$$

where $K_M \doteq 10^4\nu_o$ is approximated as a constant. For the laminar model $K_M = 0$ and for the turbulent atmosphere $\nu_o$ may be neglected compared to $K_M$. Therefore, similarity requires that

$$[U_oL_o/\nu_o]_{\text{model}} = [U_oL_o/K_M]_{\text{atm}} \tag{15}$$

For the case at hand $(L_o)_{\text{model}} = 10^{-4}(L_o)_{\text{atm}}$ and $K_M \doteq 10^4\nu_o$ so that Eq. 15 is satisfied if $U_o$ is approximately equal for the two flow systems. The approximation of representing the turbulent atmosphere as a highly viscous homogeneous fluid is appropriate for determination of the nonuniform mean motion $\bar{U}_i$ as controlled by complex topography. In essence, the turbulent shear stress at the topographic surface is replaced by an equivalent viscous shear stress for comparison with the laminar flow model.

When similarity of the mean flow has been achieved, parallel reasoning leads to the conclusion that the mean concentration field $\bar{\chi}$ will also be similar. The dimensionless turbulent diffusion equation with the turbulent transport terms approximated by $K_c\partial\bar{\chi}/\partial x_i$ has the form

$$\partial\bar{\chi}^*/\partial t^* + \bar{U}_j^*\partial\bar{\chi}^*/\partial x_j^* = [(k_c/U_oL_o) + (K_c/U_oL_o)]\partial^2\bar{\chi}^*/\partial x_j^*\partial x_j^* \tag{16}$$

For the laminar model $K_c = 0$ and for the turbulent prototype $K_c \gg k_c$. Therefore, when

$$(\bar{U}_j^*)_{\text{model}} = (\bar{U}_j^*)_{\text{atm}}$$

similarity of $\bar{\chi}^*$ will be assured if

$$[U_oL_o/k_c]_{\text{model}} = [U_oL_o/K_c]_{\text{atm}} \tag{17}$$

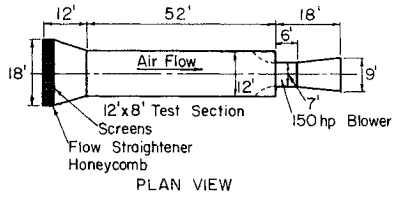


**Fig. 2 Environmental wind tunnel.**

Equation 17 is approximately satisfied for the flow being considered since $L_{\text{model}} = 10^{-4}L_{\text{atm}}, K_c \doteq 10^4k_c$ and $U_o$ is the same order of magnitude for each flow.

## III. Laboratory Facilities

Neglecting the requirement of Rossby number equality, the essential requirements in addition to those usually required for an aeronautical-type wind tunnel are as follows:

1) Develop gross Richardson numbers comparable to those formed in the atmosphere—$(-0.5 \leq Ri \leq 0.5)$, 2) Develop thick (2–3 ft) momentum and thermal boundary layers by natural momentum and heat transfer to surface over which flow occurs, and 3) Develop a zero pressure gradient in the direction of mean flow.

The first requirement is attainable in a recirculation-type wind tunnel by making provisions for heating (cooling) the wind-tunnel floor while cooling (heating) the air during its return to the test section. This capability must be accompanied by the ability to operate at low-wind speeds—down to 0.5 fps. Requirement two is best accomplished through use of a long test section. By this approach the thick shear layer will have the appropriate mean velocity, mean temperature and turbulence structure to meet the requirements for approach flow similarity. Requirement three can be met in the most versatile way by providing cross-sectional area adjustment. A flexible ceiling mounted on hangers of adjustable length provide a workable system.

Details for meeting these requirements are given by Cermak[20] and Plate and Cermak.[21] Figure 1 gives plan and elevation views of the completed facility.

The ambient level of turbulence in the meteorological wind tunnel is exceptionally low at a value of 0.05%. Stable air flow can be maintained at any selected value in the range of 0.5–100 fps. Ambient air temperature may be controlled to ±0.5°C over the range of 5°–95°C while the lower boundary may be maintained at any temperature in the range 5°–200°C. When the boundary is smooth, values of $\delta$ and $\delta_T$ are nearly equal over the downstream end of the thermally controlled surface. Values of $\delta$ and $\delta_T$ approach 3 ft when $U_o$ is approximately 6 fps.

For studies in which thermal stratification is not essential but thick boundary layers are necessary, a nonrecirculating wind tunnel such as the one shown in Fig. 2 can be used.

Recent studies have been made by Counihan[10] and Ludwig and Sundaram[22] on artificial thickening of turbulent boundary

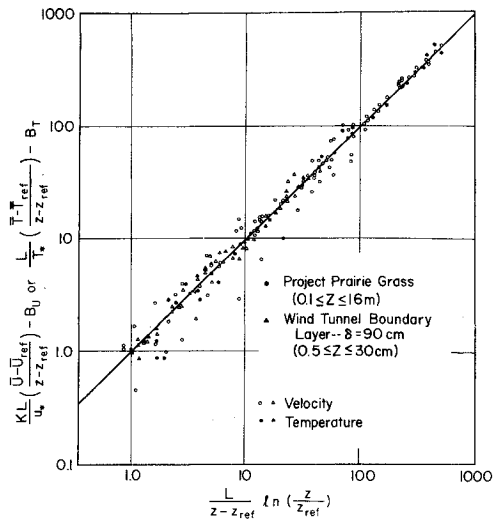


**Fig. 3 Comparison of mean velocity and mean temperatnre profiles measured in the wind tunnel and the atmosphere.[24]**

layers by longitudinal vortex generators and trip fences placed at the test-section entrance. The boundary-layer structure obtained in this manner appears to be similar to naturally developed boundary-layer structure and $\delta$ can be doubled for the same test-section length. Therefore, the possibility exists for simulation of neutral atmospheric boundary layers in conventional wind tunnels. Banks of graded grids, screens, stacked plates, and honeycombs of continuously varying thickness have been utilized to obtain the desired mean velocity profiles; however, these methods give no control of the turbulence structure.

Development of a facility which can provide flow characteristics developed by the wind tunnel shown in Fig. 1 and also simulate Coriolis-acceleration effects remains a challenge to experimentalists.[23]

## IV. Atmospheric Boundary-Layer and Diffusion Simulations

In this section data obtained from the meteorological wind tunnel and from the atmosphere will be compared for micro-, small-, and meso-scale phenomena. Several examples of simulated flow and diffusion over urban areas and complex topography are described.

### Micro-Scale Flow Structure

Measurements of boundary-layer structure have been made by Chuang and Cermak[24] and Arya and Plate[25] in the meteorological wind tunnel 27 m downwind from the test section entrance. At this section boundary-layer char-

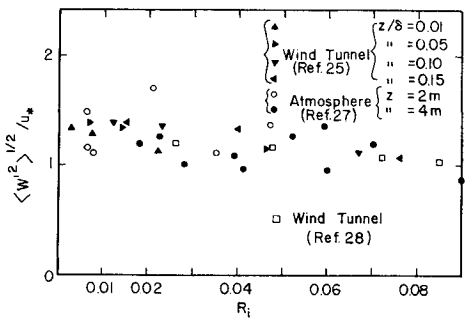


**Fig. 4 Vertical velocity fluctuations for stably stratified wind tunnel and atmospheric boundary layers.**

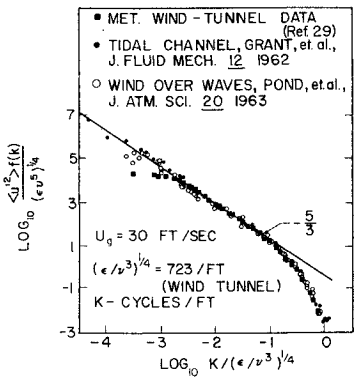


**Fig. 5 Longitudinal turbulence spectra for laboratory and geophysical shear flows.**

acteristics change very slowly with distance and planar homogeneity is approximated closely in the lower 15% of the boundary layer. Mean air velocity and temperature are compared with atmospheric-surface-layer data taken from the Project Prairie Grass measurements[26] on the basis of the log-linear relationships given by Eqs. (9) and (10). Figure 3 provides a comparison of these data for which $U_o$ varied from 3–10 fps with temperature differences $\Delta\bar{T}_o$ sufficient to give a Richardson number range from −0.5–0.5. These data are well represented by the log-linear relationship but more significant is the fact that the laboratory and atmospheric data show a common behavior. In stably stratified flow $B_v \doteq 10$ and in mildly unstable flow $B_U \doteq 1.5$.

Vertical velocity fluctuations have been measured in the meteorological wind tunnel and the atmosphere.[25,27,28] Root-mean-square values scaled according to the Monin-Obukhov similarity (Eq. 11) are presented in Fig. 4. Data from the atmosphere and laboratory follow the same trends and are scaled equally well with the velocity scale $u_*$ and the Monin-Obukhov length $L$.

Longitudinal one-dimensional energy spectra measurements for a thermally neutral flow in the meteorological wind tunnel have been made by Sandborn and Marshall.[29] These measurements were made for flow over a smooth boundary at the downstream end of the test section at a distance above the boundary of $\delta/2$. In Fig. 5 data from the atmosphere and ocean are shown with wind-tunnel data scaled by the Kolmogorov velocity and length scales according to Eq. (12).

Excellent agreement of the three sets of data is seen to exist down to a wave number of approximately 0.005 $(\epsilon/\nu^3)^{1/4}$. Similarity of the turbulence structure is implied for high wave numbers with a loss of similarity below a wave number determined by the wind-tunnel dimensions. Additional research on increasing the turbulent energy at small wave numbers by means of large-scale disturbances introduced at the test-section entrance is needed.

### Small-Scale Flow and Diffusion Characteristics

Small-scale atmospheric motion includes flow over cities, around man-made structures, over small topographic features, and across agricultural fields less than 10 miles in extent. Insufficient information exists to formulate any general statements about such flows; therefore, simulation can be of particular value when the details of flow through a city are needed. Some vertical distributions of mean velocity over portions of San Francisco[30] (1:200 scale) and Pittsburgh[31] (1:400 scale) are compared with measurements from a tower in the suburbs of Philadelphia.[32] These measurements are shown in Fig. 6 along with distributions of the type given by Eq. (13) commonly accepted for flows over cities.[18] The agreement between distributions of wind speed for the atmosphere and laboratory over complex surfaces such as a city is sufficient to make the simulated flow completely acceptable for the study of wind forces on structures or the advective transport of contaminants introduced from indus-

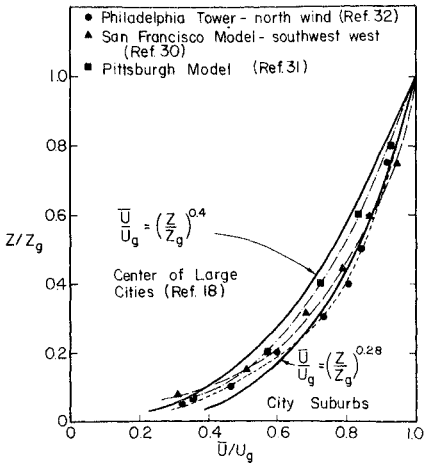


**Fig. 6 Comparison of mean velocity profiles over cities in strong winds.**

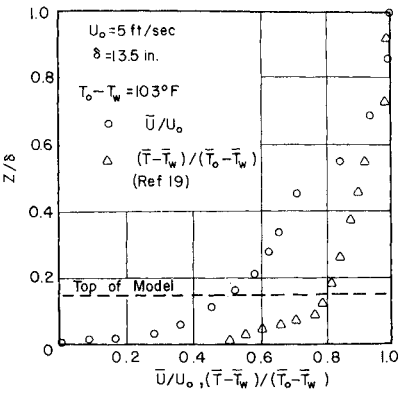


**Fig. 8 Vertical distributions of mean velocity and temperature for flow upwind of Pt. Arguello model.**

trial plant chimneys or by automobiles in the streets. Figure 7 illustrates the use of a 1:400 scale model to study the latter problem.

Many wind-tunnel studies of flow and diffusion around buildings and downstream from stacks have been made.[33,34] Comparisons of diffusion near a structure in the atmosphere and its model have been made by Halitsky[35] and Martin.[36] Taking into account the incomplete sampling of particulates in the field study, Halitsky arrived at the conclusion that the concentration fields were similar.

Diffusion characteristics in the atmosphere surface layer[26] and the wind-tunnel boundary layer for short distances downwind of a point source over a plane boundary[37,38] have been compared. The comparison of ground-level maximum concentration decay with distance was made on the basis of Eq. (14). The data from both the atmosphere and the laboratory exhibit similar behavior for short distances downwind from the source.

### Meso-Scale Flow and Diffusion Characteristics

Simulation of atmospheric motions on a scale ranging from 5–50 miles have been limited to the special but technically important case of stably stratified flows over surfaces of complex topography. In this case, the laminar flow model on scales of 1:10,000 gives useful information on such phenomena as advective dispersion[19] and mountain lee-wave structure.[39] Essential criteria for simulation of this type are given by Eqs. (15) and (17) when Richardson number equality can be achieved.

A 1:12,000 scale model study of flow and diffusion over Pt. Arguello, California[19] conducted in the wind tunnel shown in Fig. 1 provides an example of meso-scale simulation. In this application the approach flow to the model developed mean velocity and temperature profiles as shown in Fig. 8. The resulting Richardson number was about 0.2 and compared favorably with typical atmospheric flows approaching Pt. Arguello over the Pacific Ocean.

Figure 9 is a visualization of flow over the model. Strong advective dispersion occurs where the surface flows induced by the topographic features are normal to the mean flow direction. A comparison of ground-level winds observed over the site by constant-level balloons and over the model by smoke tracers is made in Fig. 10. The effects of Honda Canyon and Tranquillion Ridge are common to flow at both scales.

A point source of fluorescent particles in Honda Canyon was used to determine transport characteristics in the field. Lines of samplers at ground level collected cross-wind dosages at four distances downwind. The field source was simulated in the model by release of helium from a point source and ground-level samples were collected at the corresponding downwind positions. In Fig. 11 the maximum ground-level concentration is plotted as a function of distance downwind from the source. The concentration scales were shifted to bring the data points into coincidence; therefore, only the relative concentrations are of significance. However, the relative decrease in concentration is the same in both the model and prototype for the same relative change in distance. This finding is in agreement with the arguments leading to Eqs. (15) and (17).

## V. Summary

The turbulent atmospheric boundary layer can be simulated in long test-section wind tunnels with the exception of effects caused by Coriolis acceleration. Rotational effects can be simulated in special rotating flow systems; however, existing systems are too limited in scale to satisfy the boundary-value similarity requirements for near planar-homogeneity as is found in the atmosphere. Fortunately, experi-

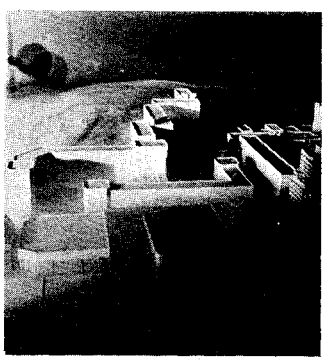

**Fig. 7 Visualization of advective transport through proposed urban renewal project for Denver—stably stratified flow from left to right.**

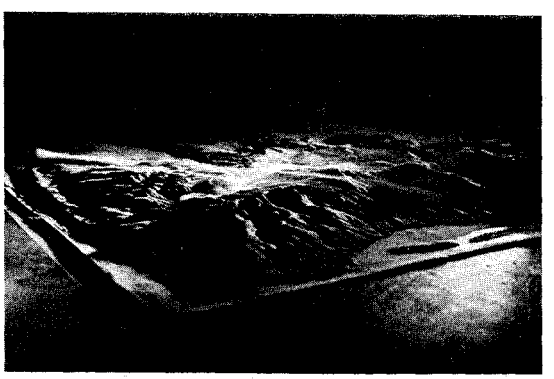

**Fig. 9 Visualization of advective dispersion over Pt. Arguello by stably stratified laminar flow.**

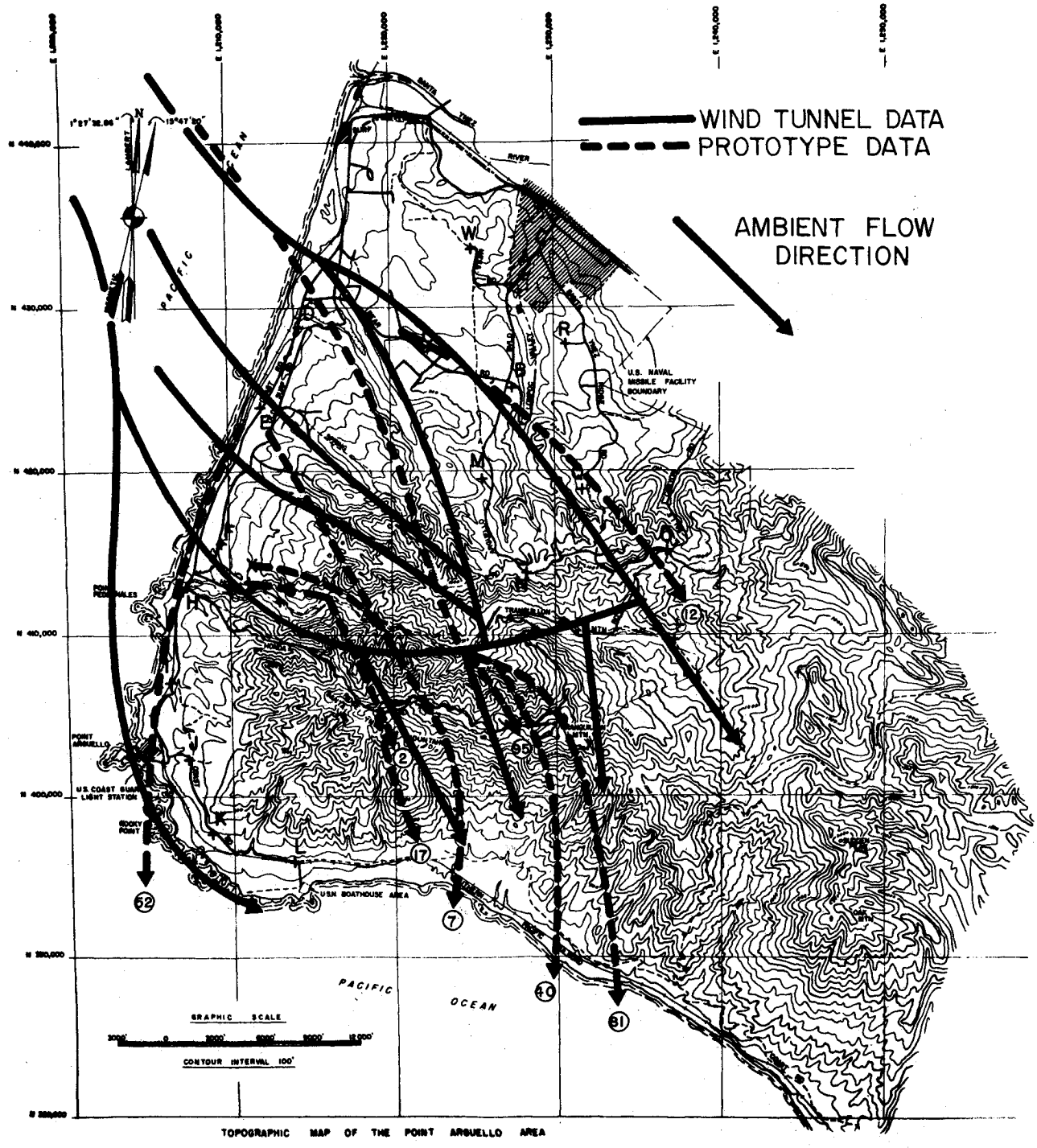


**Fig. 10 Ground-level winds for stably stratified flow over Pt. Arguello (1:12,000 scale).**

mental data from the laboratory and the atmosphere do not show evidence of measurable differences in surface-layer turbulence structure as a result of Coriolis acceleration in the atmosphere.

Time averages of micro-scale features within the lower 15% of thermally stratified turbulent boundary layers formed in wind tunnels are in excellent agreement with corresponding data measured within the atmospheric surface layer. This agreement is restricted to boundary layers formed over a sufficiently long boundary to produce near planar-homogeneity within the simulated surface layer. A precise statement on the required boundary length to produce the necessary degree of planar-homogeneity for similarity at micro-scales cannot be given without further research. However, the length of 70–90 ft yields data which agree with atmospheric data well within the errors of measurement when scaled with the Monin-Obukhov length and velocity scales. The same statement can be made for turbulence spectra down to a wave number determined by the boundary-layer thickness when scaled with the Kolmogorov length and velocity scales.

The mean velocity distribution of turbulent boundary layers over modeled areas of the Earth several miles in extent (small-scale) when covered by high roughness elements such as the buildings of a city are in good agreement with the atmospheric counterparts. This is the case when geometric similarity is preserved, the Reynolds number is sufficiently large to guarantee invariance of flow patterns over sharp

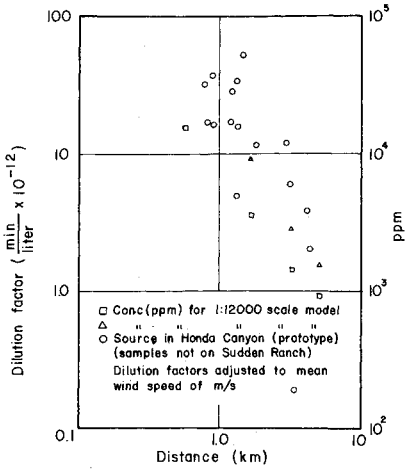


**Fig. 11 Attenuation of maximum ground-level concentrations downwind from point source over model and prototype of Pt. Arguello.**

edged buildings and the approach flow is similar to the atmospheric boundary layer. Under these conditions, the turbulence structures are expected to be similar also; however, essentially no turbulence data have been obtained in the atmospheric boundary layer over a city to check this expectation.

Laboratory studies of atmospheric motions near the Earth's surface at meso-scales require use of models about 10,000 times smaller than the prototype surface features. In this case, Reynolds-number differences are so large that similarity in the ordinary sense does not exist. An approximate similarity of flow in the friction layer can be obtained at this scale for a stably stratified atmosphere over complex terrain. In this case, a laminar flow structure dominated by the surface geometry is obtained in the wind tunnel. Such a flow is observed to be approximately similar in mean velocity to the turbulent prototype flow. The similarity is a result of the turbulent atmosphere behaving approximately as a highly viscous fluid when observed on a scale many times the integral scale of turbulence.

Simulated atmospheric boundary layers may be employed profitably in a number of ways. From a long-range point of view, the most important utilization is for basic research on the structure of turbulence and diffusion in thermally stratified atmospheric surface layers. However, an equally valuable use is for the study of specific environmental problems. A multitude of different problems have been studied experimentally in simulated atmospheric boundary layers. However, the most exciting and perhaps the most important applications for the future, are studies to obtain data for planning and design. Air flow and diffusion resulting from different arrangements of streets, freeways and tall buildings in urban renewal projects or new city plans; diffusion from sources in existing cities to provide information for strategic control measures during adverse meteorological conditions; and determination of wind forces and dynamic responses of proposed high-rise structures are examples of such studies.

## References

[1] Lettau, H. H. and Dabbert, W. F., "Vari-angular Wind Spirals," *Boundary-Layer Meteorology*, Vol. 1, No. 1, March 1970, pp. 40–60.

[2] Lumley, J. L. and Panofsky, H. A., *"The Structure of Atmospheric Turbulence,"* Wiley, New York, 1964,

[3] Monin, A. S. and Yaglom, A. M., *"Statistical Hydromechanics, Part I: The Mechanics of Turbulence,"* Nauka Press, Moscow, 1965; English translation by Joint Publications Research Service, U.S. Department of Commerce.

[4] Cermak, J. E. and Arya, S. P. S., "Problems of Atmospheric Shear Flows and Their Laboratory Simulation," *AGARD Conference Proceedings No. 48*, 1970, pp. 12.1–12.16.

[5] Cermak, J. E., "Determination of Wind Loading on Structural Models in Wind-Tunnel Simulated Winds," *Proceedings of the Symposium on Wind Effects on High-Rise Buildings*, Northwestern Univ., Evanston, Ill., March 1970, pp. 61–88.

[6] Sadeh, W. Z., Cermak, J. E., and Kawatani, T., "Flow Over High Roughness Elements," *Boundary-Layer Meteorology*, Vol. 1, 1971, pp. 321–344.

[7] Cermak, J. E., Orgill, M. M., and Grant, L. O., "Laboratory Simulation of Atmospheric Motion and Transport Over Complex Topography as Related to Cloud Seeding Operations," *Proceedings of the Second Conference on Weather Modification*, pp. 59–65.

[8] Monin, A. S. and Obukhov, A. M., "Fundamentale Geselzmässigheiten der Turbulenten Vermischung in der Bodennahem Schicht der Atmosphäre," *Akademiia Nauk SSSR. Geofizicheskii Institut. Trudy*, Vol. 151, No. 24, 1954, p. 163.

[9] Cermak, J. E., et al., "Simulation of Atmospheric Motion by Wind-Tunnel Flows," Rept. CER66JEC-SI17, 1966, Fluid Dynamics and Diffusion Lab., Colorado State Univ., Fort Collins, Colo.

[10] Counihan, J., "A Method of Simulating a Neutral Atmospheric Boundary Layer in a Wind Tunnel," *AGARD Conference Proceedings No. 48*, 1970, pp. 14.1–14.13.

[11] Hidy, G. M., "On Atmospheric Simulation: A Colloquium," NCAR-TN-22, 1966.

[12] McVehil, G. E., Ludwig, G. R., and Sundaram, T. R., "On the Feasibility of Modeling Small Scale Atmospheric Motions," Rept. ZB-2328-P-1, April 1967, Cornell Aeronautical Lab., Buffalo, N.Y.

[13] Méry, P., "Reproduction en Similitude de la Diffusion dans la Couche Limite Atmosphérique," La Houille Blanche, Vol. 3169, 1969, pp. 327–344.

[14] Panofsky, H. A., "The Structure of Atmospheric Shear Flows—A Review," *AGARD Conference Proceedings No. 48*, 1970, pp. 1.1–1.12.

[15] Kolmogorov, A. N., "The Local Structure of Turbulence in an Incompressible Fluid for Very Large Wave Numbers," *Proceedings (Doklady) Academy of Sciences, USSR*, Vol. 30, 1941, pp. 301–305.

[16] Cermak, J. E., "Lagrangian Similarity Hypothesis Applied to Diffusion in Turbulent Shear Flow," *Journal of Fluid Mechanics*, Vol. 15, No. 1, 1963, pp. 49–64.

[17] Jensen, M., "The Model-Law for Phenomena in Natural Wind," *Ingeniorøn-International Edition*, Vol. 2, No. 4, 1958, pp. 121–128.

[18] Davenport, A. G., "The Treatment of Wind Loading on Tall Buildings," *Proceedings of the Symposium on Tall Buildings*, Pergamon Press, New York, 1966, pp. 441–456.

[19] Cermak, J. E. and Peterka, J., "Simulation of Wind Field Over Point Arguello, California by Wind-Tunnel Flow Over a Topographic Model," Rept. CER65JEC-JAP64, 1966, Fluid Dynamics and Diffusion Lab., Colorado State Univ., Fort Collins, Colo.

[20] Cermak, J. E., "Wind Tunnel for the Study of Turbulence in the Atmospheric Surface Layer," Rept. CER58JEC42, 1958, Fluid Dynamics and Diffusion Lab., Colorado State Univ., Fort Collins, Colo.

[21] Plate, E. J. and Cermak, J. E., "Micro-meteorological Wind Tunnel Facility," Rept. CER63EJP-JEC9, 1963, Fluid Dynamics and Diffusion Lab., Colorado State Univ., Fort Collins, Colo.

[22] Ludwig, G. R. and Sundaram, T. R., "On the Laboratory Simulation of Small-Scale Atmospheric Turbulence," Rept. VC-2740-S-1, Dec. 1969, Cornell Aeronautical Lab. Inc., Buffalo, N.Y.

[23] Caldwell, D. R. and Van Atta, C. W., "Some Measurements of Instabilities and Turbulence in Ekman-Boundary Layers," *AGARD Conference Proceedings No. 48*, 1970, pp. 22.1–22.13.

[24] Chuang, H. and Cermak, J. E., "Similarity of Thermally Stratified Shear Flows in the Laboratory and Atmosphere," *Proceedings of an International Symposium on Boundary Layers and Turbulence with Geophysical Applications* published in *The Physics of Fluids*, Vol. 10, Pt. II, No. 9, Sept. 1967, pp. S255–S258. Intern. Union for Radio Science and Intern. Union for Geodesy and Geophysics.

[25] Arya, S. P. S. and Plate, E. J., "Modeling of the Stably Stratified Atmospheric Boundary Layer," *Journal of Atmospheric Science*, Vol. 26, No. 4, July 1969, pp. 656–665.

[26] Barad, M. L., ed., "Project Prairie Grass—A Field Program in Diffusion," Geophysical Research Paper 59, 1958, Geophysical Research Directorate, Bedford, Mass.

[27] Mordukovich, M. I. and Tsvang, L. R., "Direct Measurement of Turbulent Flows at Two Heights in the Atmospheric Ground Layer," Izvestia Atmospheric and Oceanic Physics, Vol. 2, 1966, pp. 477–486.

[28] Cermak, J. E. and Chuang, H., "Vertical Velocity Fluctuations in Thermally Stratified Shear Flows," *Proceedings International Colloquium on Atmospheric Turbulence and Radio Wave Propagation*, Intern. Union for Radio Science and Intern. Union for Geodesy and Geophysics, Publishing House "Nauka," Moscow 1965, pp. 93–104.

[29] Sandborn, V. A. and Marshall, R. D., "Local Isotropy in Wind-Tunnel Turbulence," U.S. Army Grant TR DA-AMC-28-043-64-G-9, Oct. 1965, Fluid Dynamics and Diffusion Lab., Colorado State Univ., Fort Collins, Colo.

[30] Marshall, R. D. and Cermak, J. E., "Wind Studies of Bank of America World Headquarters Building, Part II, Wind-Tunnel Study" Technical Report CER66-67RDM-JEC19, Fluid Dynamics and Diffusion Lab., Colorado State Univ., Fort Collins, Colo., Oct. 1966.

[31] Davenport, A. G. and Isyumov, N., "A Wind-Tunnel Study for the United States Steel Building," Engineering Science Research Report BLWT-5-67, Nov. 1967, The University of Western Ontario.

[32] Slade, D. H., "Wind Measurements on a Tall Tower in Rough and Inhomogeneous Terrain," *Journal of Applied Meteorology*, Vol. 8, No. 2, April 1969, pp. 293–297.

[33] Ukeguchi, N., Sakata, H., Okamoto, H., and Ide, Y., "Study of Stack Gas Diffusion," Technical Bulletin No. 52, August 1967, Mitsubishi Heavy Industries, Ltd.

[34] Strom, G. H. and Halitsky, J., "Important Consideration in the Use of the Wind Tunnel for Pollution Studies of Power Plants," *Transations of the ASME*, Vol. 77, No. 6, 1955.

[35] Halitsky, J., "Validation of Scaling Procedures for Wind Tunnel Model Testing of Diffusion Near Buildings," Rept. TR-69-8, Geophysical Sciences Lab. New York Univ., Dec. 1969.

[36] Martin, J. E., "Correlation of Wind Tunnel and Field Measurements of Gas Diffusion Using Krypton 85 as a Tracer," Michigan Memorial Phoenix Project Rept. 272, June 1965, Univ. of Michigan.

[37] Wieghardt, K., "Über Ausbreitungsvergänge in Turbulenten Reibungsschichten," *Zeitschrift Für Angewandte Mathematik und Mechanik*, Vol. 28, 1948, pp. 346–55.

[38] Davar, K. S., "Diffusion from a Point Source Within a Turbulent Boundary Layer," Ph.D. Dissertation, Fluid Mechanics Program, College of Engineering, Colorado State University, Fort Collins, Colo., 1961.

[39] Lin, J. T. and Binder, G. J., "Simulation of Mountain Lee Waves in a Wind Tunnel," Technical Rept. CER67-68JTL-GJB24, Fluid Dynamics and Diffusion Lab., Colorado State Univ., Fort Collins, Colo., Dec. 1967.

SEPTEMBER 1971 AIAA JOURNAL VOL. 9, NO. 9

# A Theory of Supersonic Flow past Steady and Oscillating Blunt Bodies of Revolution

S. S-H. CHANG*
*Lockheed Missiles & Space Company, Sunnyvale, Calif.*

**This paper presents a new method of series truncation. The technique is to locate the singularities in the complex plane and then, by using a suitable transformation, to map them away from the region of interest. The method is applied to supersonic flow over both steady and oscillating blunt bodies of revolution. The steady blunt-body solution is obtained by using an inverse method of series truncation with the computation carried out to the third truncation. The steady solution presented yields almost four-figure accuracy throughout the subsonic region, in comparison with known exact solutions. The oscillating blunt-body problem is solved by using a direct method of series truncation with the computation carried out to the second truncation. Two types of motion are considered: "plunging" oscillation and "lunging" oscillation. The oscillation amplitude is assumed to be small; otherwise, within the validity of the governing differential equations, no other restriction is made.**

## Nomenclature

$B$ = bluntness of conic section [see Eq. (1)]
$C$ = $1 - B$
$C_1, C_2$ = parameters
$F, f$ = functions associated with perturbed shock wave
$G, g$ = functions associated with perturbed body surface
$K, k$ = reduced frequency (referred to $V_\infty/R_{sk}$)
$M_\infty$ = freestream Mach number
$p$ = pressure (referred to $\rho_\infty V_\infty^2$)
$R_{sk}$ = nose radius of shock wave
$t$ = time (referred to $R_{sk}/V_\infty$)
$u, v, w$ = velocity components along $\xi$, $\eta$, $\varphi$ axes
$V$ = velocity (referred to freestream value $V_\infty$)
$x, r$ = cylindrical polar coordinates
$z$ = dependent variable [see Eq. (11)]
$\alpha$ = parameter
$\gamma$ = adiabatic exponent
$\xi, \eta, \varphi$ = curvilinear coordinate system [see Eq. (1)]
$\rho$ = density (referred to freestream value $\rho_\infty$)
$\epsilon$ = amplitude parameter

### *Superscripts and Subscripts*

$( )'$ = ordinary differentiation
$\xi, \eta, \varphi$ = partial differentiation
$b$ = body surface
$R, I$ = real part and imaginary part of complex function
$0, 0j$ = functions or parameters associated with steady solution
$1, 1j$ = functions or parameters associated with perturbed solution

Received April 13, 1970; revision received May 17, 1971. This paper is based upon the author's Ph.D. Dissertation for Stanford University, Stanford, Calif. The author wishes to express his gratitude to M. Van Dyke for his invaluable advice and discussion. The work was partially supported by the Air Force Contract F44620-69-C-0036 (DC-C-9) (MV).

* Research Specialist.